Biophysical Chemistry, 43 (1992) 81–87
Elsevier Science Publishers B.V., Amsterdam

BIOCHE 01653

Interpretation of the X-ray scattering profiles of chromatin at various NaCl concentrations by a simple chain model

Satoru Fujiwara

Department of Biophysical Engineering, Faculty of Engineering Science, Osaka University, Toyonaka, Osaka 560 (Japan)

(Received 13 November 1991; accepted in revised form 30 November 1991)

Abstract

In order to interpret the change in the X-ray scattering profiles from rat thymus chromatin, extensive model calculation was carried out. Chromatin is modelled as a string of subunits (nucleosomes) in which disorder is introduced into the positions of adjacent subunits. Disposition parameters characterizing the arrangement of subunits were estimated for various states of chromatin, so that the main feature of the scattering profiles is described. The result indicated that the structure of chromatin changes, as the NaCl concentration increases, from the extended "beads-on-a string" structure to the condensed helical structure. The latter has an outer diameter of about 26 nm with 3–4 nucleosomes per turn. In the intermediate state, it has a loose helical structure. The estimation of disorder suggested that the arrangement of subunits is appreciably disordered even in the condensed helical filament at 50 m*M* NaCl. Our model for chromatin condensation seems to support models of the "crossed linker" type.

Keywords: X-ray scattering; Chromatin condensation; Rat thymus chromatin

1. Introduction

Chromatin, consisting of repeating units called nucleosomes, undergoes a structure change from the "10 nm" filament to the "30 nm" filament with increasing NaCl concentration of the solution [1–4]. It is important to investigate the nucleosome arrangement in a chromatin filament in various structural states, in order to understand the condensation mechanism of chromatin. The scattering profiles of chromatin in the uncondensed and the condensed states were analyzed by Bordas et al. [5] in terms of radius, pitch, and number of subunits per turn of regular helix. An irregular nature of the structure is often suggested [2,5–7]. Since interactions between adjacent nucleosomes seem to be the driving force of the structure change [8], the irregularity should be described by disorder introduced into the relationship between adjacent nucleosomes. Such a type of disorder is called a distortion of the second kind [9]. An alternative approach to emphasize the irregular nature is to describe the chromatin structure as a worm-like chain, as was done in Ref. [6]. The latter approach, however, is not admitted because the scattering maximum at about 0.045 nm^{-1} cannot be reproduced [10].

Correspondence to: Dr. S. Fujiwara, Department of Biophysical Engineering, Faculty of Engineering Science, Osaka University, Toyonaka, Osaka 560 (Japan).

In this paper, we consider a chain consisting of identical subunits, which correspond to nucleosomes, as a model for chromatin. We attempt to simulate the change observed in the X-ray scattering profiles of rat thymus chromatin, presented in a preceding paper [4]. The arrangement of subunits in the chain is characterized by parameters describing the relative positions of adjacent subunits. We introduce the disorder in considering models which, as a result, lead to structures with distortions of the second kind. The models were investigated such that the radius of gyration of the cross-section (R_c), which is estimated from the calculated profiles, and the position and the height of the peak in the calculated profiles agree with those of the experimental profiles. From the result of the model calculation, we simulate the changes of the nucleosome arrangement in the chromatin filament upon addition of NaCl.

2. Methods

2.1 The description of the model

A chromatin filament is modelled as a chain consisting of N identical subunits. The parameters are r_a, the distance between adjacent subunits, θ_a, the bond angle formed between three successive subunits, and φ_a, the dihedral angle between the planes defined by three successive subunits. To introduce (as a first approximation) isotropic distribution of adjacent subunits, a Gaussian function with a zero mean and a standard devition of Δ is used. The model is illustrated in Fig. 1.

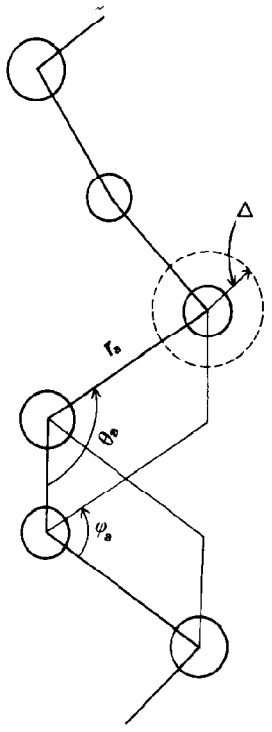

Fig. 1. The schematic picture of the model. Circles represent subunits, and Δ denotes the standard deviation of a Gaussian function. Parameters are defined in the text.

2.2 Calculation of scattering profiles

In the scattering profiles of chromatin, a peak is observed in the region of $0.03 < S < 0.1$ nm^{-1} [4] ($S = 2 \sin \theta/\lambda$, where 2θ denotes the scattering angle and λ the wavelength of X-ray). The peak is attributable to interference of nucleosomes in the filament [11]. The region in which the peak is observed is such a small-angle region that the nucleosomes can be assumed to be nearly spherically symmetric. Under this assumption, scattering intensity of the filament can be written by using Debye's formula [12] as

$$I(S) = I_s(S)\left\{N + 2\sum\sum_{j>k}\frac{\sin 2\pi S r_{jk}}{2\pi S r_{jk}}\right\} \quad (1)$$

where $I_s(S)$ is the scattering intensity of the subunit, and r_{jk} denotes the distance between jth and kth subunits. $I_s(S)$ is approximated by an exponential form [13] as

$$I_s(S) = I_s(0)\exp\left(-\tfrac{4}{3}\pi^2 R_g^2 S^2\right) \quad (2)$$

where $I_s(0)$ denotes the extrapolated intensity at $S = 0$, and R_g is the radius of gyration of the subunit, which is estimated to be 4.3 nm (Yamamoto et al., in preparation). Since adjacent subunits suffer from a disorder to have an isotropic Gaussian distribution, a distribution function should be incorporated into the equa-

tion. Equation (1) is consequently modified as follows.

$$I(S) = I_s(S)\left\{N + 2\sum_{j>k}\sum \exp(-4\pi^2 \times (j-k)\Delta^2 S^2)\frac{\sin 2\pi S r^a_{jk}}{2\pi S r^a_{jk}}\right\} \quad (3)$$

where r^a_{jk} denotes the average distance between jth and kth subunit, determined from the values of r_a, θ_a, φ_a. (for the derivation of eq. 3, see the Appendix).

By using eq. (3), we calculated the scattering intensity profiles of the model. The calculations were carried out by a PDP11/34 minicomputer (Digital Equipment Corp.). The profiles were calculated for various sets of parameters. Out of a number of models, selection has been made according to the following criteria: the R_c-value of the model to be within the range of the experimental value, the peak position of the calculated profile in accordance with that of the experimental profile, and the peak height.

3. Results and discussion

3.1 Calculation of the intensity profiles

The peak position of the profile is, as expected, sensitive to r_a-values [11]. Thus, the r_a-value is firstly determined. Since thickness of the filament is rather dependent on θ_a and φ_a, a search has been carried out to give a good value of R_c. Introduction of the disorder induces smearing of the calculated profiles, i.e., minima in the profiles are suppressed, and maxima at high angle, which are not observed in the experimental profiles, disappear. The standard deviation Δ is determined so that the minima are suppressed to a level comparable to the experimental profiles and that maxima at high angle disappear. The estimated values of the parameters are summarized in Table 1. The experimental and the calculated profiles of the model at various NaCl concentrations are shown in Fig. 2.

Table 1

The estimated parameters of the model [a]

[NaCl] (mM)	r_a (nm)	θ_a (degrees)	φ_a (degrees)	Δ (nm)
0	24	150	150–210 [b]	6.0
5	20	130	170–190 [b]	5.0
10	17	80	130–140, 210–230 [b,c]	4.5
25	13	80	55, 305 [c]	4.0
50	12	80	35, 325 [c]	3.5

[a] The parameters, r_a, θ_q, φ_a, Δ, are changed by 0.5 nm, 5°, 5°, 0.5 nm steps, respectively, and the scattering intensity profile is calculated for each set of the parameter values by using eq. (3). Out of many sets, the presented values are selected according to the criteria as described in the text.

[b] Within this range, the calculated intensity profiles satisfy the criteria.

[c] These two regions are related by φ_a and 360°-φ_a, indicating a left-handed and a right-handed helix, respectively.

In Fig. 2, the calculated profiles are scaled so that the R-value($=\Sigma|I_{obs}-I_{cal}|/\Sigma I_{obs}$), calculated in the region from the trough at around

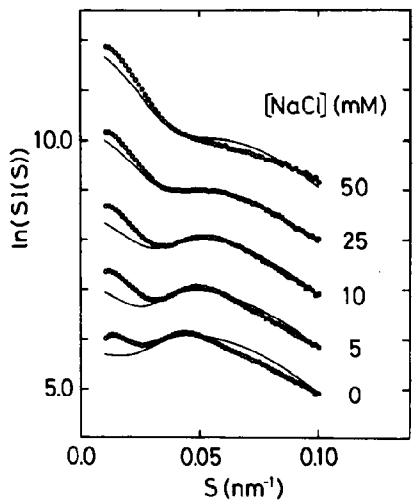

Fig. 2. The calculated and the experimental scattering intensity profiles, S vs. $\ln(SI(S))$, at various NaCl concentrations. Solid lines denote the calculated intensity profiles and open circles represent the experimental profiles. The experimental profiles are reproduction of the data presented in Fig. 3 in the preceding paper. The experimental profiles above 5 mM NaCl are displaced vertically by an arbitrary amount for clarity. The calculated profiles are scaled so that the intensity in the higher angles than the trough at about 0.03 nm^{-1} agrees with that of the experimental profiles (see text).

0.03 nm^{-1} to 0.01 nm^{-1}, is minimal. It therefore follows that intensity in the smallest-angle region of the experimental profiles is higher than that of the calculated profiles. This difference can be attributed in part to the aggregation effect of chromatin, because the experimental profiles were recorded at a chromatin concentration of 1.5 mg DNA/ml, at which aggregation of chromatin may occur [4]. The other reason comes from the component, excluded in the model. Nucleosomes in the chromatin filament are connected by the linker regions, consisting of linker-DNA of about 50 base pair (bp) length and the tail regions of histone protein H1. These linker regions also contribute to the scattering intensity. The scattering mass of the linker region is estimated to be about 20% of that of the whole nucleosome (including the linker region i.e., consisting of 196 bp DNA, two each of histones H2A, H2B, H3, H4, and a histone H1) by a similar method to that used by Koch et al. [10]. Since our model neglects the linker regions, the scattering mass of our model is lower than that of actual chromatin. This results in a reduction in intensity in the smallest-angle region. Taking these arguments into account, the main feature of the change in the intensity profiles with increasing NaCl concentration is reproduced in the calculated profiles.

Comparison of the calculated R_c and mass per unit length (M_c) values with the observed values are shown in Table 2. Since the R_c-value is one of the criteria to determine the parameters, the calculated and the observed values are identical. On the other hand, the M_c-values, estimated from the cross-sectional Guinier plots of the calculated profiles, are substantially lower than the observed values. This discrepancy seems to be due to overestimation of the observed values, as was mentioned in a preceding paper of our group [4]. Our calculated values seem to be within reasonable agreement with values observed by other investigators. For example, the M_c-value at low ionic strength is estimated to be 0.7 nucleosomes per 10 nm by Koch et al. [10], and 0.9 by Gerchman and Ramakrishnan [14]. Considering that the condensation had already proceeded to some extent under the conditions used by these researchers [4], and that they used chicken erythrocyte chromatin, which is suggested to be more "tight" than that from rat [15], the M_c-value under the low ionic condition of the present work should be lower than their values. The M_c-values in the condensed state are estimated to be around six nucleosomes per 10 nm [16,17]. Considering that the condensation is not completed at 50 mM NaCl, the calculated value at 50 mM NaCl seems to be also within a reasonable range.

Table 2

Comparison of the calculated and the observed [a] values of the radius of gyration of the cross-section (R_c) and the mass per unit length (M_c) [b] at various NaCl concentrations

[NaCl] (mM)	R_c^{cal} (nm)	R_c^{obs} (nm)	M_c^{cal}	M_c^{obs}
0	3.39–3.50 [c]	3.44±0.13	0.4	1.58±0.02
5	6.87–6.91 [c]	6.74±0.17	0.6	2.59±0.05
10	7.50–7.68 [c]	7.59±0.17	0.9	3.28±0.06
25	8.64	8.57±0.08	1.8	5.23±0.06
50	8.78	8.82±0.04	2.8	7.66±0.07

[a] The values estimated in a previous paper of our group [4].
[b] Expressed as the number of nucleosomes per 10 nm.
[c] The models with the ranges of the parameter values in Table 1 give the R_c-values within this range.

3.2 Changes of the nucleosome arrangement in chromatin filament

We discuss the changes of the nucleosome arrangement in the filament, based on the parameter values given in Table 1. At low NaCl concentrations, r_a has a large value compared with the maximum dimension of a nucleosome, 11 nm [18], which indicates the filament is rather extended. The ranges of the φ_a-value suggest that the filament has a flexible nature. The condensation along the filament axis occurs through decreases in both r_a and θ_a. Above 10 mM NaCl, φ_a has the value other than 180°, suggesting that the helical nature is introduced into the filament. Two regions, φ_a and $360° - \varphi_a$, are obtained because the X-ray scattering data cannot distinguish handedness of a helix. The values of the helical parameters above 10 mM NaCl, estimated from the values of r_a, θ_a, φ_a, are summarized in Table 3. From Table 3 it is suggested that above 10 mM

Table 3

The helical parameters estimated from the parameters of the model given in Table 1

[NaCl] (mM)	Diameter [a]	Pitch [a]	Subunits/turn
10 [b]	13.6	24.7	2.4
25	14.6	15.3	3.3
50	15.0	10.1	3.5

[a] Expressed in nm.

[b] The average values of the estimated helical parameters from the ranges of the parameter values in Table 1 are presented.

NaCl the condensation of chromatin proceeds mainly through a reduction in pitch of the helix, rather than through an increase in number of nucleosomes per turn. The helical diameter of 15.0 nm at 50 mM NaCl indicates the outer diameter of the filament is about 26 nm.

Above results have considered only regular filament structures. However, within the NaCl concentration range considered here, Δ has values which are 25–30% of the r_a-values. Computer simulation was carried out to show the chain conformations at various NaCl concentrations. The position of each subunit in the chain is defined by generating random values having Gaussian distribution with zero mean and standard deviation Δ. Typical examples of the chain conformation consisting of 70 subunits are illustrated in Fig. 3. In the absence of NaCl, a rather extended and flexible filamentous structure is seen. This "beads-on-a-string" like structure is consistent with the structure at low ionic strength suggested by Greulich et al. [6] or Koch et al. [11]. With increasing NaCl concentration, the condensation along the filament axis and appearance of local helical structure can be seen, while the flexible feature of the filament remains. The pictures in Fig. 3 are reminiscent of the flexible zig-zag structures often observed by electron microscopy, e.g. reported in Refs. [2,19,20].

Several models have been proposed for the structure of the "30 nm" filament (for a review of models, see e.g. Ref. [16]). Among these models, the solenoid model [1,2] and the models of the "crossed linker" type [5,21–23] seem most favoured [16]. The essential difference between these models is whether successive nucleosomes are in contact (the solenoid model) or not (the crossed linker model). We cannot directly compare our results with these models because our model at 50 mM NaCl might not reach the most condensed state. However, taking account of our results that condensation occurs mainly through a reduction in pitch of the helix, nucleosomes would be intercalated between successive nucleosomes in the next turn as condensation proceeds. Such a

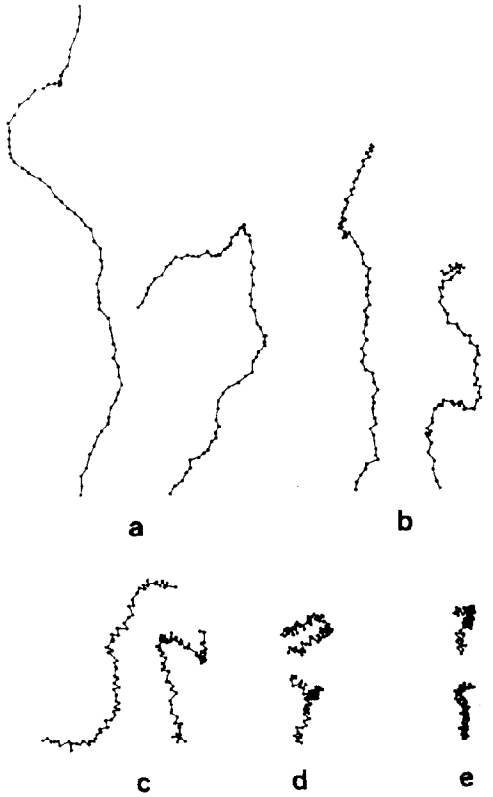

Fig. 3. Typical examples of the chain conformations generated by a computer simulation for the model of chromatin at (a) 0 mM, (b) 5 mM, (c) 10 mM, (d) 25 mM, and (e) 50 mM NaCl, respectively. Two examples of the conformations are illustrated at various NaCl concentrations. The center point of each subunit is defined by generating random values having a Gaussian distribution with zero mean and standard deviation Δ, the value estimated in Table 1. Projections to the xz-plane are illustrated of generated three-dimensional structures in which each center point of the subunit is linked by a straight line.

picture supports the models of the crossed linker type, though we cannot judge the parameter values themselves.

The existing models for the "30 nm" filament emphasize the regularity of the structure. It should be noted that the helical parameters can be defined only for a localized average structure. The filament as a whole has an irregular nature. The irregularity may derive from structural flexibility such that the local structure may vary easily according to slight changes of the environment around the chromatin filament, such as ion binding and modification of histone proteins. Such a structural flexibility may be associated with the mechanism of transcription and replication of DNA and might account for the state that no consensus on the structural details of the "30 nm" filament is obtained.

Acknowledgement

The author would like to thank Professor Tatzuo Ueki of the Institue of Physical and Chemical Research for reading the manuscript and valuable discussions. This paper is dedicated to the memory of Mr. Kenji Nakanishi and Mr. Keiji Tajima.

Appendix

Modification of Debye's formulae to include the distortion effect

Electron density of a chain which is composed of N identical subunits having isotropic electron density, can be expressed as

$$\rho(\boldsymbol{r}) = \rho_s(r) * \sum_{j=1}^{N} \delta(\boldsymbol{r} - \boldsymbol{r}_j) \qquad (A.1)$$

where $\rho_s(r)$ is the isotropic electron density of the subunit, r denotes the radial component of the vector $\boldsymbol{r}$, $*$ the convolution operation, $\boldsymbol{r}_j$ the position of jth subunit, and δ the Dirac delta function [9]. Then the scattering intensity of the chain is given by

$$I(S) = I_s(S) \times G(S) \qquad (A.2)$$

where $I_s(S)$ is the scattering intensity of the subunit, S is the radial component of the vector $\boldsymbol{S}$, and $G(S)$ is the interference function defined as

$$G(S) = \sum_j \sum_k \exp\left(2\pi \mathrm{i} \boldsymbol{S} \cdot (\boldsymbol{r}_j - \boldsymbol{r}_k)\right) \qquad (A.3)$$

where $\mathrm{i} = \sqrt{-1}$. $G(S)$ is modified to include the disorder in the relative positions of adjacent subunits. The position of jth subunit relative to kth subunit is given by

$$\boldsymbol{r}_j - \boldsymbol{r}_k = \sum_{l=k+1}^{j} \boldsymbol{r}_{l,l-1}$$

where $\boldsymbol{r}_{l,l-1}$ denotes the position of lth subunit relative to $(l-1)$th subunit and we assume $j > k$ here. Since each relative position, $\boldsymbol{r}_{l,l-1}$, fluctuates around the average position, this vector is described, by denoting the average relative position and the fluctuation as $\boldsymbol{r}^{\mathrm{a}}_{l,l-1}$ and $\Delta\boldsymbol{r}_{l,l-1}$ respectively, as $\boldsymbol{r}_{l,l-1} = \boldsymbol{r}^{\mathrm{a}}_{l,l-1} + \Delta\boldsymbol{r}_{l,l-1}$. Then

$$\boldsymbol{r}_j - \boldsymbol{r}_k = \boldsymbol{r}^{\mathrm{a}}_{jk} + \sum_{l=k+1}^{j} \Delta\boldsymbol{r}_{l,l-1} \qquad (A.4)$$

where $\boldsymbol{r}^{\mathrm{a}}_{jk}$ denotes the average position of jth subunit relative to that of kth subunit. $\Delta\boldsymbol{r}_{l,l-1}$ is assumed to have an isotropic Gaussian distribution with zero mean and standard deviation Δ for all l. Substitution of eq. (A.4) into eq. (A.3) and averaging over $G(S)$ for the distribution of $\Delta\boldsymbol{r}_{l,l-1}$, yields

$$G(S) = \sum_j \sum_k \exp\left(2\pi \mathrm{i} \boldsymbol{S} \cdot \boldsymbol{r}^{\mathrm{a}}_{jk}\right) \times \exp\left(-4\pi^2 |j-k| \Delta^2 S^2\right) \qquad (A.5)$$

The spherical average of eq. (A.5) gives

$$G(S) = \sum_j \sum_k \exp\left(-4\pi^2 |j-k| \Delta^2 S^2\right) \times \frac{\sin 2\pi S r^{\mathrm{a}}_{jk}}{2\pi S r^{\mathrm{a}}_{jk}} \qquad (A.6)$$

Simple calculation yields the spherical average of $I(S)$ given by

$$I(S) = I_s(S)\left\{N + 2\sum_{j>k}\sum \exp(-4\pi^2 \times (j-k)\Delta^2 S^2)\frac{\sin 2\pi S r_{jk}^a}{2\pi S r_{jk}^a}\right\} \quad (A.7)$$

This equation gives the scattering intensity of a chain having distortions of the second kind.

On the other hand, if a chain has distortions of the first kind, which are distortions in which long range order is retained, the scattering intensity can be expressed, by assuming that each subunit may deviate from the ideal position according to a Gaussian with zero mean and standard deviation Δ, as follows [9].

$$I(S) = I_s(S)\left\{N + 2\sum_{j>k}\sum \exp(-4\pi^2\Delta^2 S^2) \times \frac{\sin 2\pi S r_{jk}^a}{2\pi S r_{jk}^a}\right\} \quad (A.8)$$

The exponential factor in the second term of the above equation corresponds to the temperature factor in crystallographic terms. Note the difference between eqs. (A.7) and (A.8).

References

1 J.T. Finch and A. Klug, Proc. Natl. Acad. Sci. USA 73 (1976) 1899.
2 F. Thoma, T. Koller and A. Klug, J. Cell Biol. 83 (1979) 403.
3 P. Suau, E.M. Bradbury, and J.P. Baldwin, Eur. J. Biochem. 97 (1979) 593.
4 S. Fujiwara, Y. Inoko and T. Ueki, J. Biochem. 106 (1989) 119.
5 J. Bordas, L. Perez-Grau, M.H.J. Koch, M.C. Vega and C. Nave, Eur. Biophys. J. 13 (1986) 175.
6 K.O. Greulich, E. Wachtel, J. Ausio, D. Seger and H. Eisenberg, J. Mol. Biol. 193 (1987) 709.
7 J. Widom and A. Klug, Cell 43 (1985) 207.
8 J.O. Thomas and A.J.A. Khabaza, Eur. J. Biochem. 112 (1980) 501.
9 B.K. Vainshtein, Diffraction of X-rays by chain molecules (Elsevier, Amsterdam, 1966).
10 M.H.J. Koch, M.C. Vega, Z. Sayers and A.M. Michon, Eur. Biophys. J. 14 (1987) 307.
11 M.H.J. Koch, Z. Sayers, M.C. Vega and A.M. Michon, Eur. Biophys. J. 15 (1987) 133.
12 P. Debye, Ann. Phys. 46 (1915) 809.
13 A. Guinier and G. Fournet, Small angle scattering of X-rays (Wiley, New York, NY, 1955) p. 24.
14 S.E. Gerchman and V. Ramakrishnan, Proc. Natl. Acad. Sci. USA 84 (1987) 7802.
15 D.L. Bates, P.J.G. Butler, E.C. Pearson and J.O. Thomas, Eur. J. Biochem. 119 (1981) 469.
16 Z. Sayers, in: Synchrotron radiation in chemistry and biology I, ed. E. Mandelkow (Springer-Verlag, Berlin, 1988) p. 203.
17 G. Felsenfeld and J.D. McGhee, Cell 44 (1986) 375.
18 T.J. Richmond, J.T. Finch, B. Rushton, D. Rhodes and A. Klug, Nature 311 (1984) 532.
19 J.A. Subirana, S. Munoz-Guerra, J. Aymami, M. Redermacher and J. Frank, Chromosoma 91 (1985) 377.
20 C.L.F. Woodcock, L.L.Y. Frado and J.B. Rattner, J. Cell. Biol. 99 (1984) 42.
21 D.Z. Staynov, Int. J. Biol. Macromol. 5 (1983) 3.
22 V. Makarov, S. Dimitrov, V. Smirnov and I. Pashev, FEBS lett. 181 (1985) 357.
23 S.P. Williams, B.D. Athey, L.J. Muglia, R.S. Schappe, A.H. Gough and J.P. Langmore, Biophys. J. 49 (1986) 233.